Available online at www.sciencedirect.com
SCIENCE DIRECT®

Journal of Solid State Chemistry 173 (2003) 164–171

JOURNAL OF SOLID STATE CHEMISTRY

http://elsevier.com/locate/jssc

Subsolidus phase relations and crystal structures of R–Ca–Cu–O (R = Nd, Sm, Gd, Tm) systems

C.Q. Han,[a] G.B. Song,[a,b] X.L. Chen,[a] J.K. Liang,[a,c,*] and G.H. Rao[a]

[a] Center for Condensed Matter Physics, Institute of Physics, Chinese Academy of Sciences, Beijing 100080, People's Republic of China
[b] Institute of Mineral Materials and Application, Southwest University of Science and Technology, Mianyang 621002, People's Republic of China
[c] International Center for Materials Physics, Chinese Academy of Sciences, Shenyang 110016, People's Republic of China

Received 26 July 2002; received in revised form 25 September 2002; accepted 7 October 2002

Abstract

The subsolidus phase relations of R_2O_3–CaO–CuO ternary systems (R = Nd, Sm, Gd, Tm) have been investigated by X-ray powder diffraction. All samples were synthesized at about 950° in air. There exists a ternary compound $Ca_{14-x}R_xCu_{24}O_{41}$ ($x = 4$ for R = Nd, Gd and $x = 5$ for R = Sm) and a ternary solid solution $Ca_{2+x}R_{2-x}Cu_5O_{10}$ (R = Nd, Sm, Gd, Tm) with a wide composition range Δx of about 0.6. The compound $Ca_{14-x}R_xCu_{24}O_{41}$ possesses a layered orthorhombic structure and is isostructural to $Sr_{14-x}Ca_xCu_{24}O_{41}$. The lattice parameters a and c of the compound are basically independent of the ionic radius of R, while the lattice parameter b and unit-cell volume V decrease substantially with the decrease of the ionic radii of R. The $Ca_{2+x}R_{2-x}Cu_5O_{10}$ solid solution is isostructural to $Ca_{2+x}Y_{2-x}Cu_5O_{10}$, the structure of which is based on an orthorhombic "$NaCuO_2$-type" subcell containing infinite one-dimensional chains of edge-shared square planar cuprate groups crosslinked by the layered cations Ca and R that locate in the inter-chain tunnels.

Keywords: R_2O_3–CaO–CuO (R = Nd, Sm, Gd, Tm) systems; Phase relations; $Ca_{10}R_4Cu_{24}O_{41}$ (R = Nd, Sm, Gd) structure; $Ca_{2+x}R_{2-x}Cu_5O_{10}$ (R = Nd, Sm, Gd, Tm) structure

1. Introduction

After discovering high T_C oxide superconductors $La_{2-x}Ba_xCuO_4$ [1] and $YBa_2Cu_3O_{7-\delta}$ [2,3], the phase relations of a series of R–Ba–Cu–O (R = rare earth elements) systems have been extensively investigated to improve the superconducting properties and search for new superconductors, such as Y_2O_3–BaO–CuO system [4–7], La_2O_3–BaO–CuO system [8,9], Pr_6O_{11}–BaO–CuO system [10,11], Nd_2O_3–BaO–CuO system [11,12], Sm_2O_3–BaO–CuO system [13,14], Eu_2O_3–BaO–CuO system [15,16], Gd_2O_3–BaO–CuO system [17,18], Ho_2O_3–BaO–CuO system [19,20], Dy_2O_3–BaO–CuO system [19], Er_2O_3–BaO–CuO system [21], Tm_2O_3–BaO–CuO system [22] and Yb_2O_3–BaO–CuO system [23]. Meanwhile, similar investigations have been extended to some R–Sr–Cu–O systems, e.g. Y_2O_3–SrO–CuO system [24,25], La_2O_3–SrO–CuO system [26], Nd_2O_3–SrO–CuO system [27,28], Sm_2O_3–SrO–CuO system [29], Eu_2O_3–SrO–CuO system [30], Gd_2O_3–SrO–CuO system [31], Ho_2O_3–SrO–CuO system [32] and Tm_2O_3–SrO–CuO system [33]. However, only a few investigations have been performed on the phase relations of R_2O_3–CaO–CuO systems. It is known that a partial substitution of Ca for Pr in $PrBa_2Cu_3O_7$ compound has a notable influence on superconducting properties of the material. $Pr_{1-x}Ca_xBa_2Cu_3O_{7-\delta}$ synthesized under high pressure is a superconductor with $T_C = 115\,K$ [34]. This suggests that the Ca ions may play an important role in the high-temperature superconductivity of the oxide. In order to investigate the Ca^{2+} substituting effects and explore possible new functional materials, in this paper we study the phase relations and crystal structures of R_2O_3–CaO–CuO (R = Nd, Sm, Gd, Tm) systems by means of X-ray powder diffraction.

---

*Corresponding author. Center for Condensed Matter Physics, Institute of Physics, Chinese Academy of Sciences, Beijing 100080, People's Republic of China.

E-mail address: jkliang@aphy.iphy.ac.cn (J.K. Liang).

0022-4596/03/$ - see front matter © 2002 Elsevier Science (USA). All rights reserved.
doi:10.1016/S0022-4596(02)00125-1

2. Experimental

2.1. Preparation of samples

All samples were prepared by solid-state chemical reaction in air. The purity of starting materials Nd_2O_3, Sm_2O_3, Gd_2O_3, Tm_2O_3, CuO and $CaCO_3$ is higher than 99.9%. Raw powders with proper compositions were weighed, thoroughly mixed and ground in an agate mortar, and then presintered in air at 850°C for about 12 h. The presintered raw powders after regrinding and remixing were pressed into disks with diameters of 10–12 mm and thicknesses of 1–2 mm. The disks were sintered again at about 950°C for 48 h in air, and then cooled in the furnace to room temperature. The above process was repeated several times, until the homogeneity of samples was reached based on X-ray diffraction (XRD) phase identification. Care was taken for the samples rich in CaO since they were unstable and tended to form the basic calcium carbonate after absorbing carbon dioxide and water from air. After preparation, the samples must be kept in a desiccator before being used for the X-ray diffraction experiments. Thirty-eight samples for Nd_2O_3–CaO–CuO system, 57 samples for Sm_2O_3–CaO–CuO system, 45 samples for Gd_2O_3–CaO–CuO system and 46 samples for Tm_2O_3–CaO–CuO system were prepared, and their compositions are shown in Figs. 1–4, respectively.

2.2. X-ray powder diffraction analysis

XRD data were collected by a Rigaku Rint-2500 X-ray diffractometer with a power of 200 mA × 40 kV, CuKα radiation and a graphite monochromator for diffracted beam. The XRD data for structure analysis and accurate lattice parameter determination were collected in a step scan mode with a scanning step of $2\theta = 0.02°$and a sampling time of 2 s. Pure Si powder was added to the specimens as an internal standard. The data for phase identification were recorded in a continuous scan mode with a rate of 4°/min in 2θ.

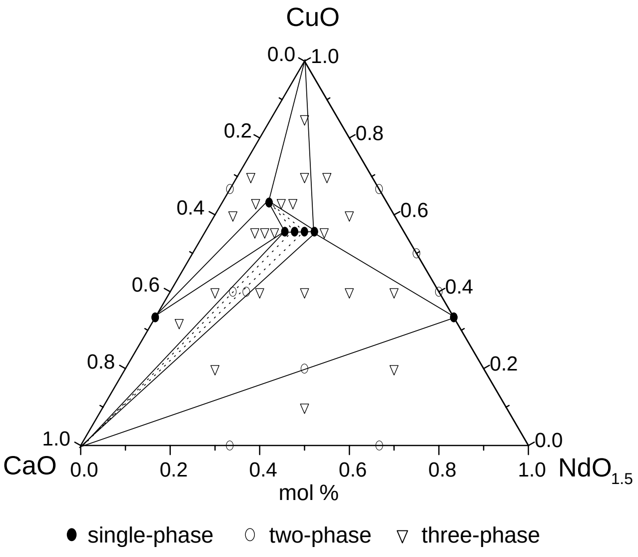

Fig. 1. The subsolidus phase relations of the $NdO_{1.5}$–CaO–CuO ternary system sintered at 950° in air.

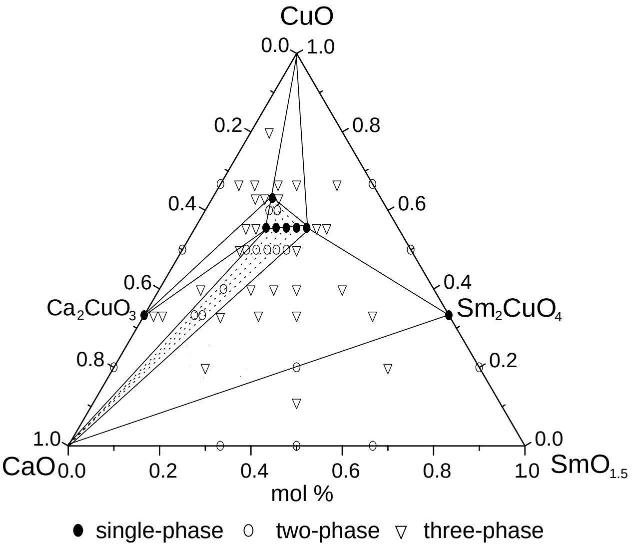

Fig. 2. The subsolidus phase relations of the $SmO_{1.5}$–CaO–CuO ternary system sintered at 950° in air.

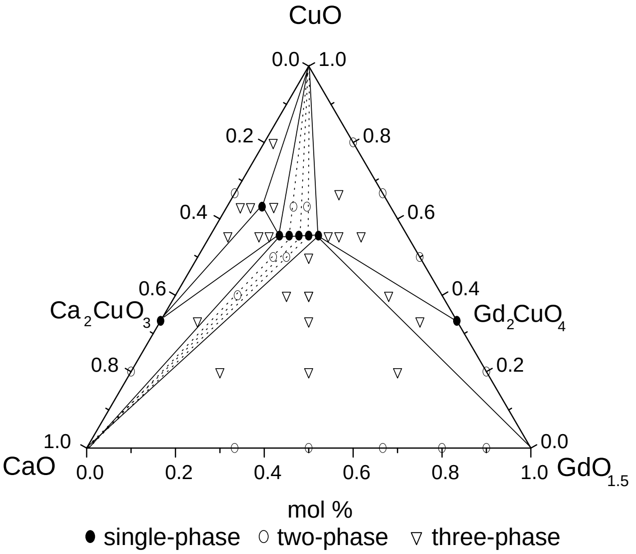

Fig. 3. The subsolidus phase relations of the $GdO_{1.5}$–CaO–CuO ternary system sintered at 950° in air.

3. Results and discussion

3.1. Relevant pseudo-binary system

3.1.1. CaO–CuO system

It was reported that there exist two compounds at room temperature in the CaO–CuO system [35]:

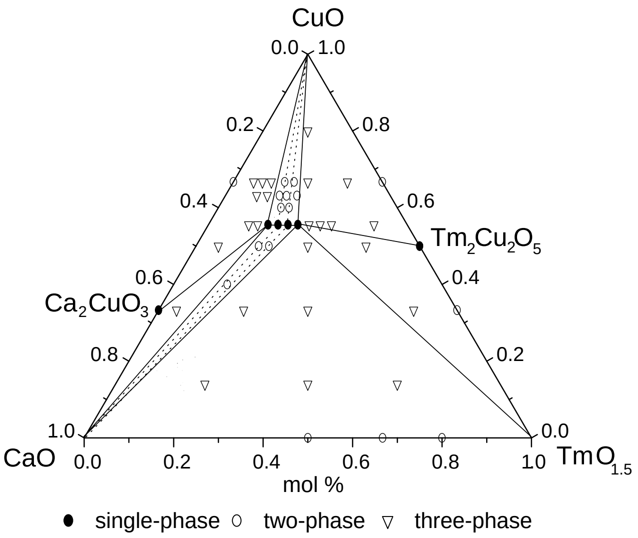

Fig. 4. The subsolidus phase relations of the $TmO_{1.5}$–CaO–CuO ternary system sintered at 950° in air.

$CaCu_2O_3$ and Ca_2CuO_3. $CaCu_2O_3$ belongs to an orthorhombic system with space group Pmmm. Its lattice parameters are $a = 9.85$ Å, $b = 4.11$ Å and $c = 3.47$ Å. Ca_2CuO_3 possesses an orthorhombic unit cell with space group *Immm*. Its lattice parameters are $a = 12.239$ Å, $b = 3.779$ Å and $c = 3.259$ Å. The compound $CaCuO_{2-\delta}$, in which the content of oxygen varies, could be synthesized under high pressure [36]. Under our experimental conditions, only one compound Ca_2CuO_3 was identified, the crystal structure of which is confirmed to be the same as reported in Ref. [35].

3.1.2. R_2O_3–CaO (R=Nd, Sm, Gd, Tm) systems

In our present investigation, no other binary compound was detected in R_2O_3–CaO (R = Nd, Sm, Gd, Tm) systems, though compounds Gd_4CaO_7 and $Tm_6Ca_2O_{11}$ with a monoclinic lattice were reported in Refs. [37, 38].

3.1.3. R_2O_3–CuO (R=Nd, Sm, Gd, Tm) systems

Only one compound R_2CuO_4 was observed in each R_2O_3–CuO (R = Nd, Sm, Gd) pseudo-binary system under our synthesis conditions. The compound R_2CuO_4 (R = Nd, Sm, Gd) has a tetragonal structure with K_2NiF_4-type structure (space group $I4/mmm$). The lattice parameters a, c and unit cell volume, V, decrease with the increase in the atomic number of rare earth (decreasing of ionic radius). The lattice parameters are $a = 3.945$ Å, $c = 12.171$ Å, $V = 189.42$ Å^3 for Nd_2CuO_4, $a = 3.915$ Å, $c = 11.972$ Å, $V = 183.50$ Å^3 for Sm_2CuO_4, and $a = 3.894$ Å, $c = 11.881$ Å, $V = 180.15$ Å^3 for Gd_2CuO_4. The derived lattice parameters are consistent with the reported values in Refs. [39, 40]. The compounds $NdCuO_2$ and $SmCuO_2$, which were synthesized under reducing atmosphere and belong to a trigonal system, had been reported in Ref. [41]. In addition, $NdCu_2O_4$ [42], $SmCu_2O_4$ [43], $GdCu_2O_4$ [43] and $Nd_2Cu_2O_5$ [44] with a monoclinic structure were also reported.

In the Tm_2O_3–CuO system, there exists one compound $Tm_2Cu_2O_5$, which belongs to an orthorhombic system with space group $Pna2_1$. The lattice parameters are $a = 10.74$ Å, $b = 3.46$ Å and $c = 12.38$ Å. The result obtained agrees with that of Ref. [45].

3.2. Subsolidus phase relations of R_2O_3–CaO–CuO (R=Nd, Sm, Gd, Tm) systems

The phase identification of samples was carried out by X-ray powder diffraction. The solid solution range was determined on the basis of the variations of lattice constants with composition. Because in these systems there does not exist any polymorphism phase transition of the ternary compounds, Figs. 1–4 represent the phase relations at 950°C as well as at room temperature.

The subsolidus phase relations of the $NdO_{1.5}$–CaO–CuO and $Sm_{1.5}$–CaO–CuO systems are shown in Fig. 1 and 2, respectively. In both systems, there exist two binary compounds (Ca_2CuO_3 and R_2CuO_4), one ternary compound $Ca_{14-x}R_xCu_{24}O_{41}$ ($x = 4$ for R = Nd, $x = 5$ for R = Sm) and one ternary solid solution $Ca_{2+x}R_{2-x}Cu_5O_{10}$ ($x = -0.2 \sim 0.4$ for R = Nd and $x = -0.15$–0.5 for R = Sm).

Fig. 3 shows the subsolidus phase relations of the $GdO_{1.5}$–CaO–CuO ternary system. Two differences from the phase relations of the $RO_{1.5}$–CaO–CuO (R = Nd, Sm) systems are observed. One is that the phase boundary between CaO and R_2CuO_4 disappears, whereas a new phase boundary between $Ca_2R_2Cu_5O_{10}$ and $GdO_{1.5}$ is present. The other is the two-phase region $Ca_{2+x}R_{2-x}Cu_5O_{10}$ + $Ca_{14-x}R_xCu_{24}O_{41}$ reduces to a tie-line, and a two-phase region $Ca_{2+x}R_{2-x}Cu_5O_{10}$ + CuO becomes apparent. These phenomena may well be related to an increased stability of the compound $Ca_2R_2Cu_5O_{10}$ with an increase in the atomic number of rare earth (i.e., decreasing the ionic radius of rare earth).

The subsolidus phase relations of the $TmO_{1.5}$–CaO–CuO ternary system are shown in Fig. 4. In this system there exists only one ternary compound $Ca_{2+x}R_{2-x}Cu_5O_{10}$ with some solid solubility. The ternary compound with the $Ca_{14-x}R_xCu_{24}O_{41}$ type structure, which was observed for R = Nd, Sm, and Gd, could not be synthesized in this system.

In most of the R_2O_3–CaO–CuO systems, there exist two ternary compounds: $Ca_{14-x}R_xCu_{24}O_{41}$ and $Ca_{2+x}R_{2-x}Cu_5O_{10}$. However, in the La_2O_3–CaO–CuO system [46] only $Ca_2LaCu_5O_{8.5}$, the structure of which is closely related to that of $Ca_{14-x}R_xCu_{24}O_{41}$, and another ternary compound $CaLa_2Cu_2O_6$, were observed, while in the Tm_2O_3–CaO–CuO system only one ternary compound $Ca_{2+x}R_{2-x}Cu_5O_{10}$ was synthesized. Based on the phase relations show in Figs. 1–4, we can see that the stability of $Ca_{14-x}R_xCu_{24}O_{41}$ increases with increasing the ionic radius of rare earth, whereas the stability of $Ca_{2+x}R_{2-x}Cu_5O_{10}$ increases with decreasing the ionic radius of rare earth.

The chemical properties of the alkaline earth oxide CaO, SrO and BaO are similar to each other, and all of them have the NaCl-type structure. But the difference in ionic radius among alkaline earth ions is salient. The ternary compounds existing in R_2O_3–BaO–CuO, R_2O_3–SrO–CuO and R_2O_3–CaO–CuO systems are obviously different. In the R_2O_3–BaO–CuO system, the main ternary compounds are $Ba_2RCu_3O_{7-\delta}$, BaR_2CuO_5, etc.; in the R_2O_3–SrO–CuO system, the main ternary compounds are $Sr_2RCu_2O_{5.5}$, $Sr_3RCu_2O_{6.5}$ and $Sr_{14-x}R_xCu_{24}O_{41}$ solid solution; but in R_2O_3–CaO–CuO systems, the main ternary compounds are $Ca_{14-x}R_xCu_{24}O_{41}$, $Ca_{2+x}R_{2-x}Cu_5O_{10}$, etc. Based on the phase relations of the R_2O_3–MO–CuO (M = Ba, Sr, Ca) systems, it is apparent that the ionic radius of alkaline earth metals plays an important role in forming rare earth ternary compounds.

3.3. Crystal structure of ternary compounds

3.3.1. Crystal structure of $Ca_{14-x}R_xCu_{24}O_{41}$ ($x = 4$ for R=Pr, Nd, Gd and $x = 5$ for R = Sm)

$Ca_{10}Pr_4Cu_{24}O_{41}$, $Ca_{10}Nd_4Cu_{24}O_{41}$, $Ca_9Sm_5Cu_{24}O_{41}$ and $Ca_{10}Gd_4Cu_{24}O_{41}$ are isostructural to $Sr_{14-x}Ca_xCu_{24}O_{41}$. They are ternary compounds since there does not exist any corresponding binary compounds $Ca_{14}Cu_{24}O_{41}$ and $R_{14}Cu_{24}O_{41}$.

The crystal structure of the ternary compound $Ca_{14-x}R_xCu_{24}O_{41}$ (R = Pr, Nd, Sm, Gd) belongs to the orthorhombic system with space group *Cccm*. The chemical formula unit per unit cell is 4, that is, a unit cell contains 40Ca + 16R + 96Cu + 164O. The lattice parameters are $a = 11.282(2)$ Å, $b = 12.449(3)$ Å, $c = 27.486(10)$ Å, $V = 3860.40$ Å^3 for $Ca_{10}Pr_4Cu_{24}O_{41}$ [47]; $a = 11.291(4)$ Å, $b = 12.403(6)$ Å, $c = 27.496(10)$ Å, $V = 3850.46$ Å^3 for $Ca_{10}Nd_4Cu_{24}O_{41}$; $a = 11.296(5)$ Å, $b = 12.259(3)$ Å, $c = 27.545(7)$ Å, $V = 3814.37$ Å^3 for $Ca_9Sm_5Cu_{24}O_{41}$; $a = 11.280(4)$ Å, $b = 12.305(5)$ Å, $c = 27.515(10)$ Å, $V = 3819.09$ Å^3 for $Ca_{10}Gd_4Cu_{24}O_{41}$. Lattice parameters a and c of $Ca_{10}R_4Cu_{24}O_{41}$ vary slightly with the ionic radius of R, while lattice parameter b and unit cell volume V decrease substantially with decrease in the ionic radius of R. The relationship between the unit cell volume and ionic radius of R is shown in Fig. 5. The unit cell volume of $Ca_9Sm_5Cu_{24}O_{41}$ is smaller than expected, which may be due to the fact that the content of rare earth ion with smaller ionic radius is higher than that in other isostructural compound $Ca_{10}R_4Cu_{24}O_{41}$.

The crystal structure of $Sr_{14-x}Ca_xCu_{24}O_{41}$ was determined on a single crystal [48]. The structure, which was described by a commensurate cell, consists of three different unit layers as shown in Fig. 6: (a) There are: a [CuO4/2 (chains)] layer containing 20Cu + 40O, (b) a [$Sr_{14-x}Ca_x$] layer containing 14Sr/Ca and (c) a [$CuO_{3/3}O_{1/2}$ (sheet)] layer containing 28Cu + 42O. The dimensions a and c of the three unit layers are the same.

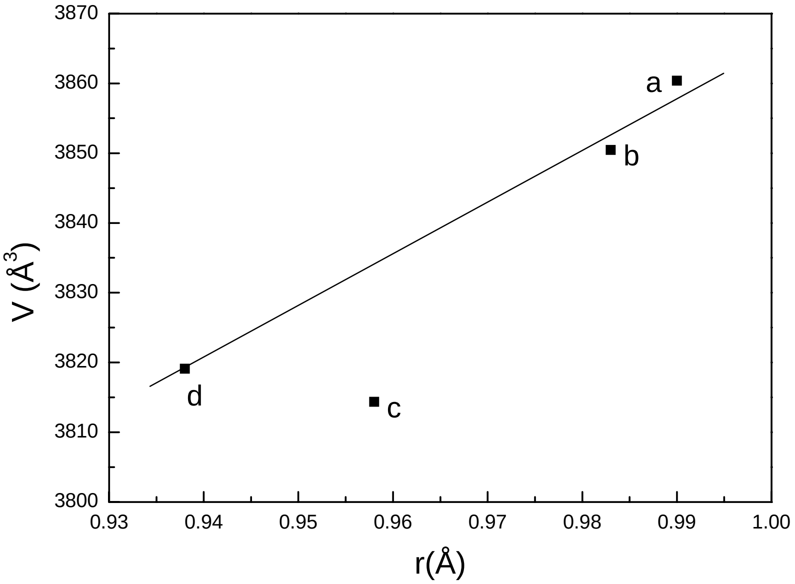

Fig. 5. Variation of the unit cell volumes of $Ca_{10}R_4Cu_{24}O_{41}$ with R-ionic radius Note: (a) $Ca_{10}Pr_4Cu_{24}O_{41}$, (b) $Ca_{10}Nd_4Cu_{24}O_{41}$, (c) $Ca_9Sm_5Cu_{24}O_{41}$, and (d) $Ca_{10}Gd_4Cu_{24}O_{41}$.

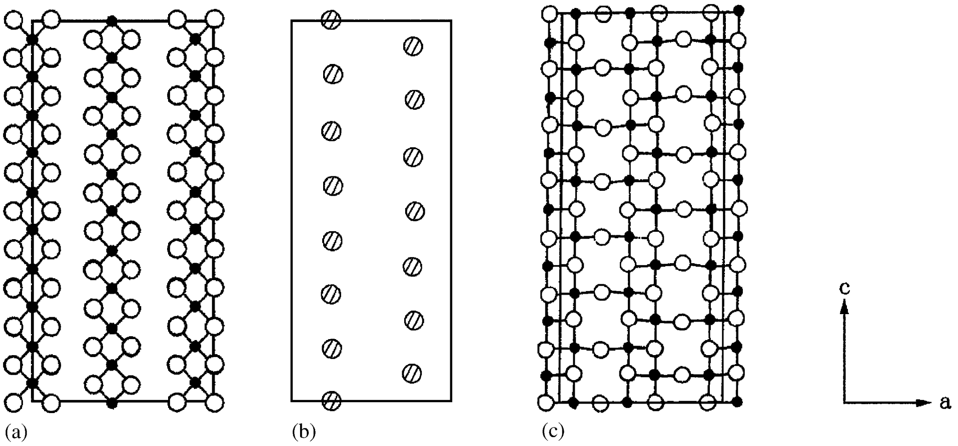

Fig. 6. Units of the layer structure of $Ca_{10}R_4Cu_{24}O_{41}$ crystal structure stacking along the *b*-axis: (a) the infinite $CuO_{4/2}$ chains propagating along the *c*-axis, (b) the [14 Ca/R] layer residing between (a) and (c) layers, (c) the [$CuO_{3/3}O_{1/2}$] sheet along the *c*-axis triple bridging oxygen, along a axis double bridging oxygen; ○—oxygen, •—copper, ⊘—calcium/rare earth.

Table 1
The subcell lattice parameters *a*, *b*, *c* and *V* of $Ca_{2+x}R_{2-x}Cu_5O_{10}$ compounds

x		−0.4	−0.2	0	0.2	0.4	0.6	0.8	1.0
a	Nd	2.8171(3)	2.8172(3)	2.8218(3)	2.8249(3)	2.8270(3)	2.8269(3)		
(Å)	Sm	2.8144(3)	2.8144(5)	2.8182(6)	2.8221(8)	2.8258(7)	2.8296(5)	2.8296(5)	
	Gd	2.8170(5)	2.8169(5)	2.8198(4)	2.8250(4)	2.8296(5)	2.8330(4)	2.8330(5)	
	Tm			2.8242(5)	2.8241(5)	2.8306(5)	2.8314(5)	2.8337(5)	2.8337(5)
b	Nd	6.3577(8)	6.3578(8)	6.3537(9)	6.3511(9)	6.3478(9)	6.3477(9)		
(Å)	Sm	6.3060(15)	6.3060(10)	6.3065(10)	6.3070(10)	6.3072(10)	6.3075(10)	6.3075(12)	
	Gd	6.2430(10)	6.2430(15)	6.2532(12)	6.2553(15)	6.2682(13)	6.2810(11)	6.2805(15)	
	Tm			6.1612(10)	6.1611(10)	6.1752(10)	6.1970(12)	6.2122(12)	6.2121(10)
c	Nd	10.704(2)	10.703(2)	10.686(2)	10.673(2)	10.659(2)	10.661(2)		
(Å)	Sm	10.667(2)	10.667(2)	10.657(2)	10.648(2)	10.638(2)	10.627(2)	10.627(2)	
	Gd	10.644(3)	10.644(4)	10.630(4)	10.624(5)	10.616(3)	10.606(2)	10.607(3)	
	Tm			10.575(2)	10.575(3)	10.568(3)	10.562(2)	10.552(3)	10.553(3)
V	Nd	191.71	191.70	191.59	191.48	191.24	191.30		
($Å^3$)	Sm	189.31	189.31	189.41	189.52	189.60	189.67	189.67	
	Gd	187.19	187.17	187.43	187.73	188.28	188.72	188.71	
	Tm			184.01	184.00	184.71	185.33	185.75	185.75

The unit cell arrangement, in order, is (a) (b) (c) (b) (*a*) (*b*) (*c*) (*b*) along the *b*-axis, and a unit cell contains 56 Sr/Ca + 96Cu + 164O or 56Ca/*R* + 96Cu + 164O. For $Ca_{10}R_4Cu_{24}O_{41}$ compounds we can see from Fig. 6 that the rare earth *R* and calcium ions occupy exclusively the (b) layer above and below the layers (a) and (c), so the size of the rare earth ions has a predominant effect on lattice parameter *b*, whereas the parameters *a* and *c* basically remain constant.

3.3.2. Crystal structure and solid solution of $Ca_{2+x}R_{2-x}Cu_5O_{10}$ (*R*=Nd, Sm, Gd, Tm)

The crystal structure of $Ca_{2+x}R_{2-x}Cu_5O_{10}$ (*R* = Nd, Sm, Gd, Tm) is an incommensurate one based on the orthorhombic $NaCuO_2$ type subcell. Davies [49] described the structure of $Ca_2R_2Cu_5O_{10}$ (*R* = Y, Nd, Gd) in detail, and deduced the relationship between the incommensurate orthorhombic subcell and commensurate superstructure with an orthorhombic or a monoclinic system. We determined the crystal structure of the $Ca_2Pr_2Cu_5O_{10}$ on the basis of a monoclinic commensurate superstructure [47]. The structure of $Ca_{2+x}R_{2-x}Cu_5O_{10}$ consists of infinite one-dimensional chains of edge-shared square planar cuprate groups crosslinked by the layered cations Ca and *R*, which occupy the sites in the inter-chain tunnels.

The solid solutions of $Ca_{2+x}R_{2-x}Cu_5O_{10}$ (*R* = Nd, Sm, Gd, Tm) were formed over a wide composition range. The lattice parameters *a*, *b*, *c* and unit cell volume *V* of $Ca_{2+x}R_{2-x}Cu_5O_{10}$ subcell vary with the composition (*x*) as shown in Table 1. The homogeneous range of

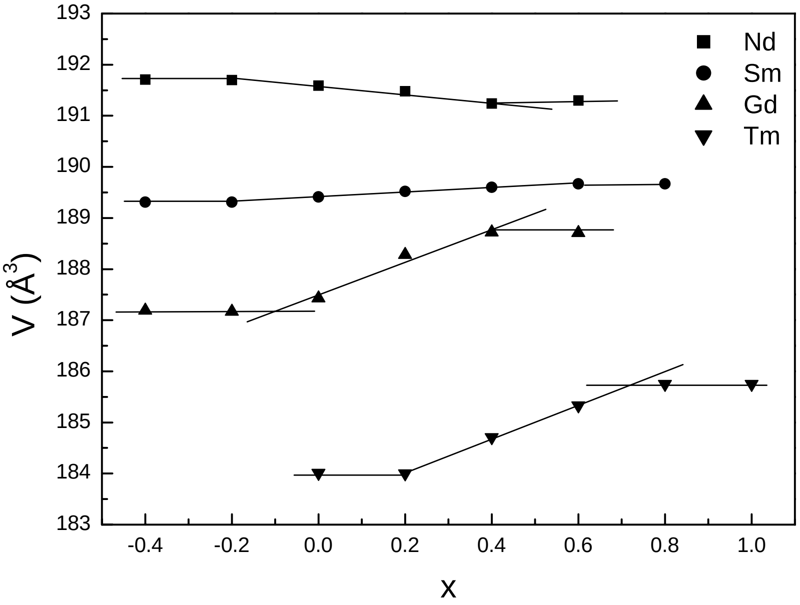

Fig. 7. The variation of the subcell volume in the $Ca_{2+x}R_{2-x}Cu_5O_{10}$ solid solutions with compositions x.

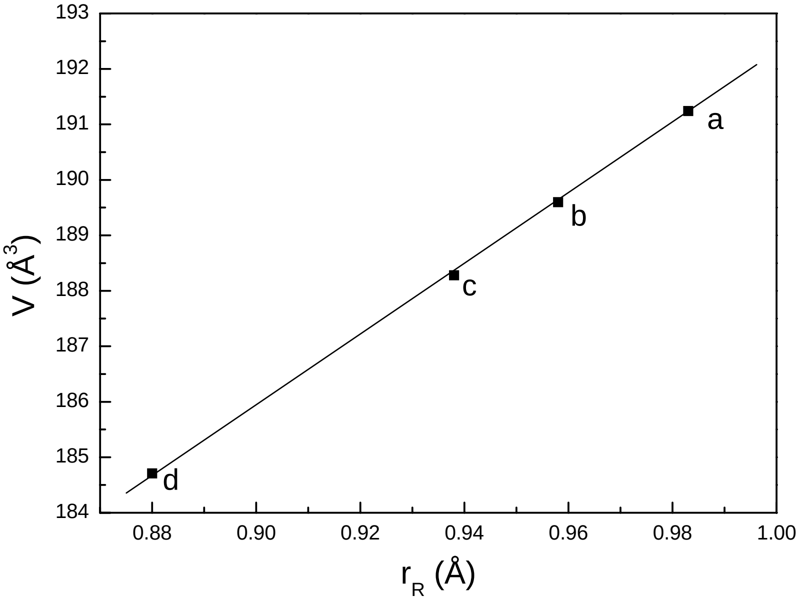

Fig. 8. The variation of the unit cell volume with the radius of the rare earth ions r_R (Å) for single phase $Ca_{2+x}R_{2-x}Cu_5O_{10}$ at $x=0.4$. Note: (a) $Ca_{2.4}Nd_{1.6}Cu_5O_{10}$, (b) $Ca_{2.4}Gd_{1.6}Cu_5O_{10}$, (c) $Ca_{2.4}Sm_{1.6}Cu_5O_{10}$ and (d) $Ca_{2.4}Tm_{1.6}Cu_5O_{10}$.

the $Ca_{2+x}R_{2-x}Cu_5O_{10}$ solid solution was determined according to the relationship of lattice parameters with composition. In a single-phase region, the variation of lattice parameters with the composition is linear, whereas in the multiphase region the lattice parameters remain constant. The variation of subcell volume with the content of rare earth ion x is shown in Fig. 7, from which we can derive the homogeneous range of the $Ca_{2+x}R_{2-x}Cu_5O_{10}$ ($R=$Nd, Sm, Gd, Tm) solid solutions as follows:

$$Ca_{2+x}Nd_{2-x}Cu_5O_{10}, \quad x = -0.2-0.4,$$
$$Ca_{2+x}Sm_{2-x}Cu_5O_{10}, \quad x = -0.15-0.5,$$
$$Ca_{2+x}Gd_{2-x}Cu_5O_{10}, \quad x = -0.1-0.4,$$
$$Ca_{2+x}Tm_{2-x}Cu_5O_{10}, \quad x = 0.2-0.74,$$

The homogeneous range of $Ca_{2+x}R_{2-x}Cu_5O_{10}$ solid solutions, Δx, is roughly all about 0.6 for different rare earth ions, but the solid solution region shifts to the calcium-ion-rich side with the decrease in the ionic radius of the rare earth. Assuming that $Ca_{2+x}R_{2-x}Cu_5O_{10}$ compounds are electrically neutral and all ions possess their normal valence, compounds $Ca_2R_2Cu_5O_{10}$ are stoichiometric, those with $x>0$ are oxygen-deficient compounds $Ca_{2+x}R_{2-x}Cu_5O_{10-\delta}$, and those with $x<0$ are calcium-deficient compounds $Ca_{2+x-\delta}R_{2-x}Cu_5O_{10}$.

From Fig. 7 we can see that the subcell volume in the homogeneous solid solution region of $Ca_{2+x}R_{2-x}Cu_5O_{10}$ decreases with the increase of the rare earth content for R=Nd, and with the decrease of the rare earth content for R=Sm, Gd, Tm. It shows that the effective radius of Ca, the practical radius of ions in the structure, is slightly larger than that of Sm and smaller than that of Nd. This result is in agreement with that of Ref. [49]. However, with the stoichiometric formula $Ca_2R_2Cu_5O_{10}$, (i.e. $x = 0$) we did not observe a turning point of subcell volume, although it was observed in Ref. [49].

Table 1 shows that the effect of rare earth ions on lattice parameter *a, b, c* of $Ca_{2+x}R_{2-x}Cu_5O_{10}$ solid solution is anisotropic. For $Ca_{2+x}Nd_{2-x}Cu_5O_{10}$ solid solution, as the Nd content x increases, the lattice parameters a and c increase, but the lattice parameter b and subcell volume V decrease. For $Ca_{2+x}R_{2-x}Cu_5O_{10}$ (R=Sm, Gd, Tm) solid solution, as the R content x increases, the lattice parameters *a, b* and subcell volume V increase, but the lattice parameter c decreases. The variation of the subcell volume with the ionic radius $\boldsymbol{r}_R$ of the rare earth at $x=0.4$, which sits in the single phase region for all rare earth ions, is shown in Fig. 8. The change of the subcell volume with the ionic radius of the rare earth exhibits a linear relationship, indicating the size of the rare earth ions plays an important role.

Acknowledgments

This work was supported by State Key Project on Fundamental Research in China and National Science Foundation of China.

References

[1] J.G. Bednorz, K.A. Muller, Z. Phys. B: Condens. Matter 64 (1986) 189.
[2] C.W. Chu, P.H. Hor, R.L. Meng, L. Gao, Z.J. Huang, Science 235 (1987) 567.
[3] Z.X. Zhao, L.Q. Chen, Q.S. Yang, Y.Z. Huang, G.H. Chen, R.M. Tang, G.R. Liu, Kexue Tongbao 32 (1987) 681.
[4] D.G. Hinks, L. Soderholm, D.W. Capone II, J.D. Jorgensen, I.K. Schuller, C.U. Segre, K. Zhang, J.D. Grace, Appl. Phys. Lett. 50 (1987) 1688.
[5] K.G. Frase, D.M. DeLeeuw, C.A.H. Amutsaers, C. Langereis, H.C.A. Smooren-Burg, P.J. Roommers, Physica C 152 (1988) 39.
[6] G.C. Che, J.K. Liang, W. Chen, Q.S. Yang, G.H. Chen, Y.M. Ni, J. Less-Common Met. 138 (1988) 137.
[7] K. Osamura, W. Zhang, Z. Metallkde 82 (5) (1991) 408.
[8] C. Dong, J.K. Liang, G.C. Che, S.S. Xie, Z.X. Zhao, Q.S. Yang, Y.M. Ni, G.R. Liu, Int. J. Modern Phys. B 1 (1987) 323.
[9] G.C. Che, J.K. Liang, W. Chen, S.S. Xie, Y.D. Yu, Z.X. Zhao, Q.S. Yang, G.H. Chen, Kexue Tongbao 32 (1987) 1094.
[10] J.K. Liang, X.L. Chen, X.T. Wang, W. Chen, Z. Chen, Z.Y. Qiao, Y.L. Zhang, S.S. Xie, Y.M. Ni, Solid State Commun. 76 (1990) 903.
[11] S.A. Hodorowicz, J. Czerwonka, H.A. Eick, J. Solid State Chem. 88 (1990) 391.
[12] S.J. Fu, S.S. Xie, J.K. Liang, G.C. Che, Z.X. Zhao, Mod. Phys. Lett. B 2 (1988) 1073.
[13] J. Czerwonka, H.A. Eick, J. Solid State Chem. 90 (1991) 69.
[14] Z.Y. Qiao, W.X. Yuan, X.R. Xing, Sh.K. Wei, X.R. Cheng, X.L. Chen, J.K. Liang, J. Rare Earths 11 (1993) 152.
[15] S.A. Hodorowicz, A. Lasocha, W. Lasocha, H.A. Eick, J. Solid State Chem. 75 (1988) 270.
[16] C.N. Pieczulewski, J.E. McAdams, T.O. Mason, J. Amer. Ceram. Soc. 73 (10) (1990) 3088.
[17] J.K. Liang, X.T. Xu, G.H. Rao, S.S. Xie, X.Y. Shao, Z.G. Duan, J. Phys. D 20 (1987) 1324.
[18] S.A. Hodorowicz, A. Chodorowicz-Bak, J. Czerwonka, E. Hodorowicz, W. Lasocha, H.A. Eick, J. Solid State Chem. 92 (1991) 480.
[19] Y.L. Zhang, J.K. Liang, X.R. Cheng, G.H. Rao, H.B. Liu, Y.M. Ni, D.N. Zeng, S.S. Xie, J. Less-Common Met. 146 (1989) 121.
[20] E. Hodorowicz, S.A. Hodorowicz, W.K. Wong-Ng, J. Solid State Chem. 98 (1992) 181.
[21] S.A. Hodorowicz, A. Chodorowicz-Bak, J. Czerwonka, E. Hodorowicz, W. Lasocha, H.A. Eick, Acta Phys. Polon. A75 (1989) 121.
[22] E. Hodorowic, S.A. Hodorowicz, H.A. Eick, Physica C 158 (1989) 395.
[23] J.K. Liang, X.L. Chen, X.T. Wang, W. Chen, Z. Chen, Z.Y. Qiao, Y.L. Zhang, S.S. Xie, Solid State Commun. 74 (1990) 509.
[24] R.S. Roth, C.J. Rawn, J.D. Whitler, C.K. Chiang, W.K. Wong-Ng, J. Am. Ceram. Soc. 72 (3) (1989) 395.
[25] F. Wu, S.S. Xie, Z. Chen, J.K. Liang, J. Mater. Sci. 27 (11) (1992) 3082.
[26] D.M. De Leeuw, C.A.H.A. Mutsaers, G.P.J. Geelen, C. Langereis, J. Solid State Chem. 80 (1989) 276.
[27] Ph. Labbe, H. Ledesert, V. Caignaert, B. Raveau, J. Solid State Chem. 91 (1991) 362.
[28] X.L. Chen, J.K. Liang, C. Wang, G.H. Rao, X.R. Xing, Z.H. Song, Z.Y. Qiao, J. Alloys Compd. 205 (1994) 101.
[29] C.Q. Han, X.L. Chen, J.K. Liang, G.H. Rao, J. Alloys Compd. 314 (2001) 301.
[30] C.Q. Han, X.L. Chen, J.K. Liang, Q.L. Quan, G.H. Rao, J. Solid State Chem. 156 (2001) 247.
[31] C.Q. Han, Y. Gao, X.L. Chen, J.K. Liang, G.H. Rao, J. Alloys Compd. 321 (2001) 54.
[32] W. Wong-Ng, J. Dillingham, L.P. Cook, J. Solid State Chem. 149 (2000) 333.
[33] C.Q. Han, X.L. Chen, J.K. Liang, Q.L. Quan, Y. Chen, G.H. Rao, J. Alloys Compd. 309 (2000) 95.
[34] Z.X. Zhao, K.Q. Li, G.C. Che, Physica C 341–348 (2000) 331–334.
[35] C.L. Teske, H. Muller-Buschbaum, Z. Anorg. Allg. Chem. 370 (1969) 134.
[36] N. Kobayashi, Z. Hiroi, M. Takano, J. Solid State Chem. 132 (1997) 274.
[37] I.V. Spitsin, M.L. Kovba, L.N. Lykova, V.K. Belskii, Dokl. Akad. Nauk SSSR 271 (1983) 1142.

[38] W. Muschick, H. Muller-Buschbaum, Z. Naturforschung. B 32 (1997) 495.
[39] H. Mueller-Buschbbaum, W. Wollschlager, Z. Anorg. Allg. Chem. 414 (1975) 76.
[40] P. Vigoureux, M. Braden, A. Gukasov, W. Paulus, P. Bourges, A. Cousson, D. Petitgrand, P. Adelmann, G. Heger, M. Meven, J.P. Lauriat, S.N. Barilo, D.I. Zhigunov, Physica C 273 (3–4) (1997) 239.
[41] H. Haas, E. Kides, Z. Kristallogr. Kristallgeom. Kristallphys. Kristallchem. 129 (1969) 250.
[42] B.H. Chen, D. Walker, E.R. Suard, B.A. Scott, Chem. Mater. 7 (1995) 355.
[43] J.L. Luce, A.M. Stacy, Chem. Mater. 9 (1997) 1508.
[44] J.M.S. Skakle, A.R. West, J. Mater. 5 (1995) 765.
[45] J.L. Garcia-Munoz, J. Rodriguez-Carvajal, J. Solid State Chem. 115 (1995) 324.
[46] Q. Zhong, Y.L. Zhang, X.L. Chen, G.H. Rao, J.K. Liang, J. Alloys Compd. 210 (1994) 261.
[47] C.Q. Han, G.B. Song, X.L. Chen, J.K. Liang, G.H. Rao, J. Alloys Compd., submitted for publication.
[48] E.M. McCarron, M.A. Subramanian, J.C. Calabrese, R.L. Harlow, Mater. Res. Bull. 23 (1988) 1355.
[49] P.K. Davies, J. Solid State Chem. 95 (1991) 365.